Domes of trachydacitic and rhyolitic volcanism: Mount Amiata complex and lunar highland domes.

By Raffaello Lena (text and images) and Guy Heinen (mineral microscopy)

Introduction

In previous works I have described the Strombolian eruptions, which may have formed the largest dark mantle deposits on the Moon, and the Plinian eruptions including the Vesuvius volcano.
Stromboli and Vesuvius are two steep stratovolcanoes and are explosive. These volcanoes have higher proportion of silica minerals and more gas in the magma.
In comparison the lunar mare domes have moderate or gentle slopes caused by fluid lava flows of basaltic composition.
On the other hand the highland lunar domes (e.g. Gruithuisen domes) originated from highly silicic more viscous non-mare lavas, likely dacitic or rhyolitic in composition.
Some candidates for localities where the lunar silicic rocks occur have been identified from remote sensing data sets that combine infrared spectroscopy, gamma-ray spectroscopy, and topography. Gruithuisen highland domes have infrared spectra indicating silica-rich compositions (as described below) and thus originated from dacitic to rhyolitic volcanism.

Lava flows and chemical composition

Basaltic lava flows easily because of low viscosity. The low viscosity is due to low silica content. Andesitic magma erupts explosively because it tends to have higher gas content. Higher viscosity is related to higher silica content.
The table below describes the average composition in SiO_2 for different types of lavas.

	Basalt	Andesite	Trachyte	Dacite	Rhyolite
% SiO_2	**49.20**	**57.94**	**61.21**	**65.01**	**72.82**

Trachyte contains 60 to 65% silica content, thus less SiO_2 than rhyolite and more Na_2O and K_2O than dacite. These chemical differences account for the feldspar-rich mineralogy of the rock type. The mineralogical composition of rhyolite is defined as containing mostly quartz and feldspar with a total silica content of more than 69%. Quartz in rhyolite may be usually present in amounts of 25% to 30%. Feldspars often comprise 50% to 70% of rhyolite.

Rhyolitic magma erupts catastrophically because rhyolitic lava has high gas content. It is viscous and therefore traps gas, builds pressure and explosively erupts. High viscosity is related to highest silica content.

Lunar highland domes

Gruithuisen highland domes are known to have large diameters of up to 20 km, heights of more than 1000 m, steep flank slopes between 7° and 10°, and very high edifice volumes of several hundred km^3 (Lena et al., 2013). Wilson and Head (2003) show that while the eruption processes that formed Gruithuisen δ (termed G2) and the Northwest Dome (termed G3) occurred over more than 20 years at low effusion rates, between 6 and 50 m^3s^{-1}, the effusion rate was 119 m^3s^{-1} for Gruithuisen γ (termed G1) over a period of 38 years.
The lava that formed the Gruithuisen highland domes had high viscosities (between 10^8 and 10^9 Pa s). The assumed source region is the lower lunar crust. These domes for their steep slope angles display a long shadow if imaged under oblique solar illumination (Figs. 1-2).

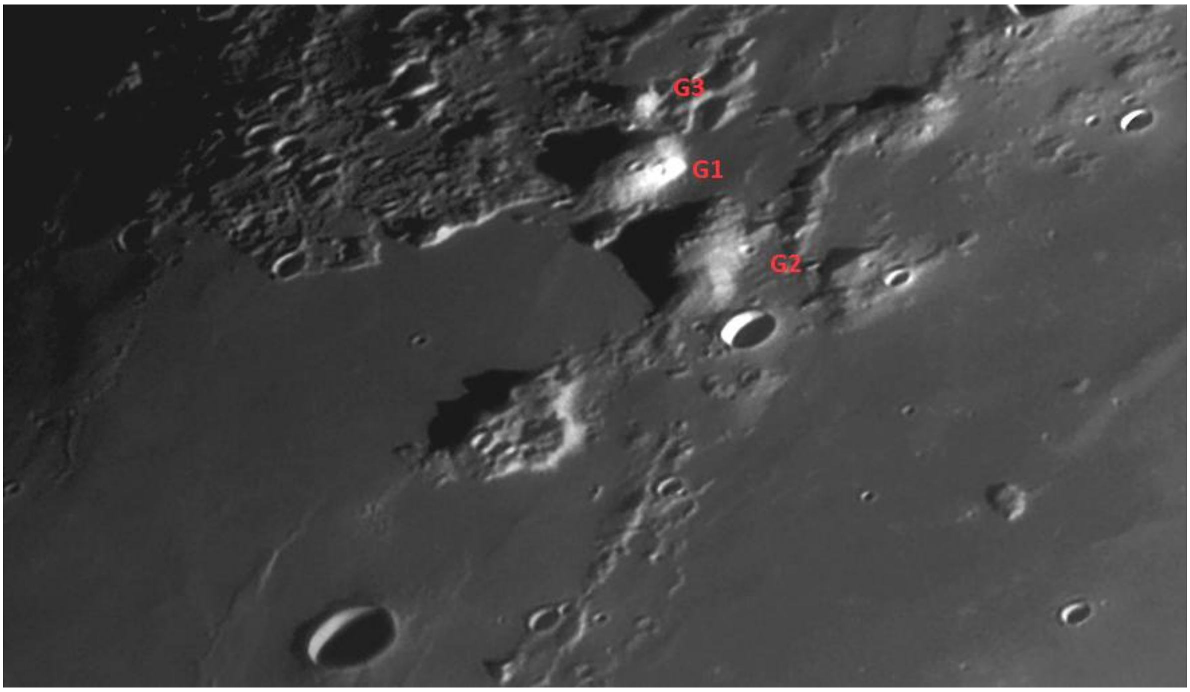

Figure 1: The Gruithuisen domes closed at the terminator. Image made by Paolo Lazzarotti on December 1, 2006, at 21:58 UT with a Gladius CF 315.

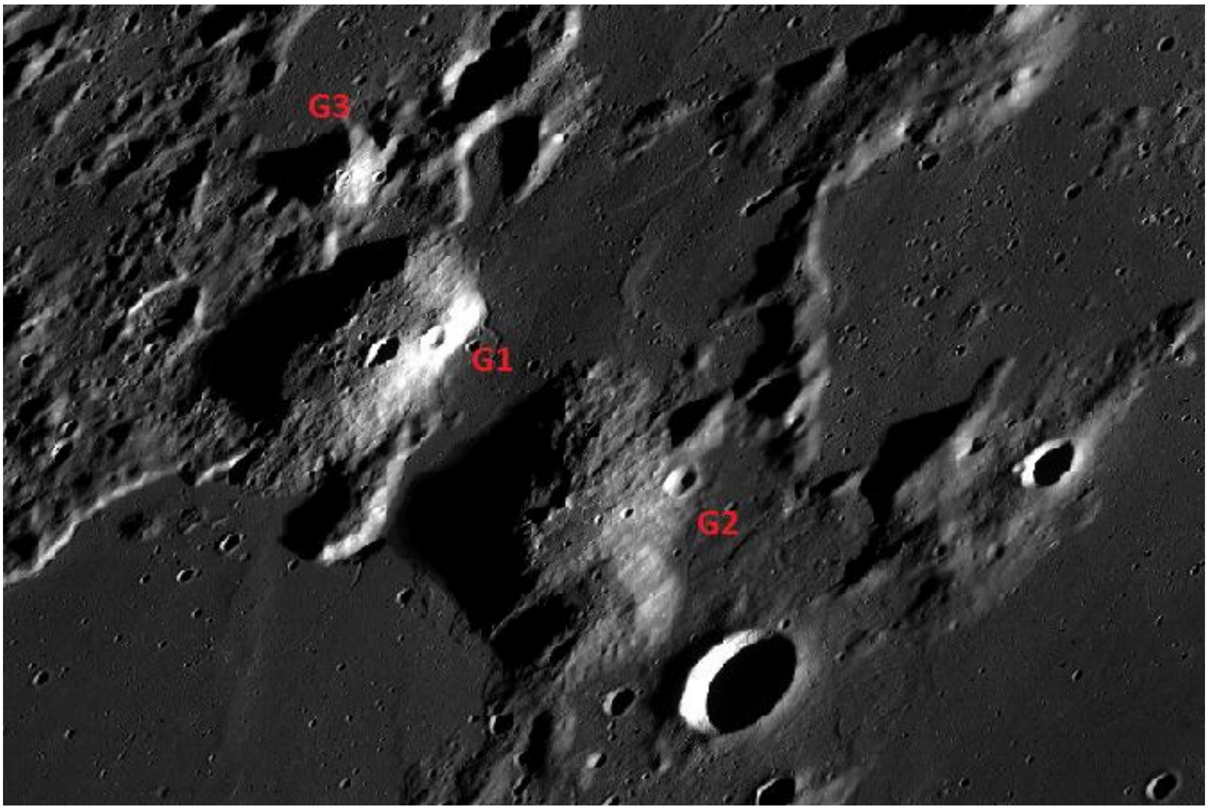

Figure 2: WAC imagery of the Gruithuisen domes G1-G3.

The height of Gruithuisen γ (G1) is of 1740 m, the diameter amounts to 19 km, resulting in an average slope of 8.3°. The height of Gruithuisen δ and the Northwest Dome (G2 and G3) amounts to 1960 m and 1117 m respectively, with diameters of 27 km and 7.5 km, resulting in average slopes of 6.9° (G2) and 9.1° (G3). Figure 3 displays the profiles of Griuthuisen domes based on GLD100 dataset.

The edifice volumes assuming a parabolic shape of the domes is determined to 247 km³, 544 km³ and 43 km³, respectively.

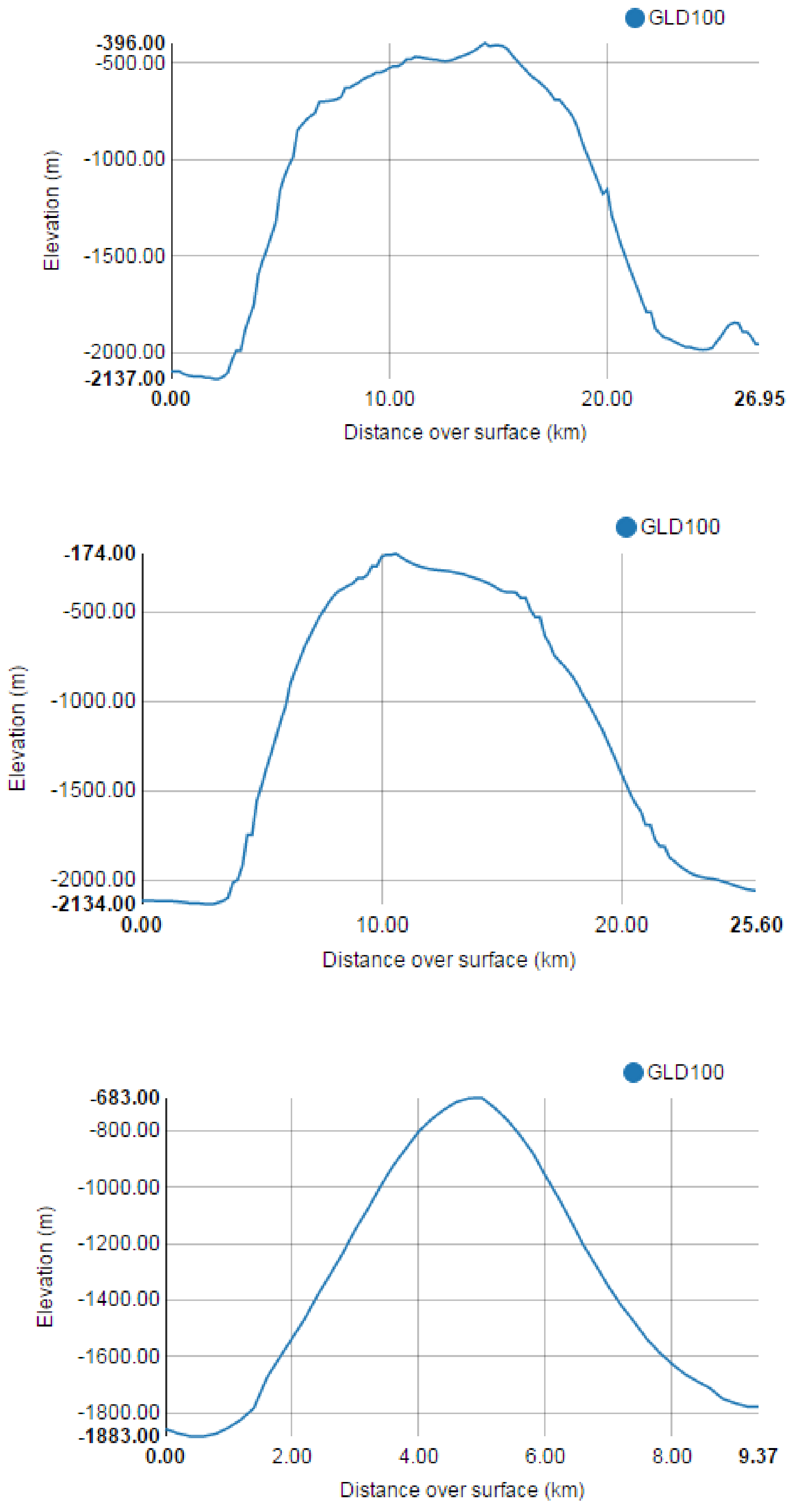

Figure 3: Sectional profile in E-W direction of the highland domes. Top: G1. Middle: G2. Bottom: G3. G1 height GLD100 dataset 1740 m, G2 height GLD100 dataset 1960 m, G3 height measured based with GLD100 dataset amounts to 1117 m.

The 3D reconstruction (Fig. 4-5) is obtained using WAC mosaic draped on top of the global WAC-derived elevation model (GLD100).

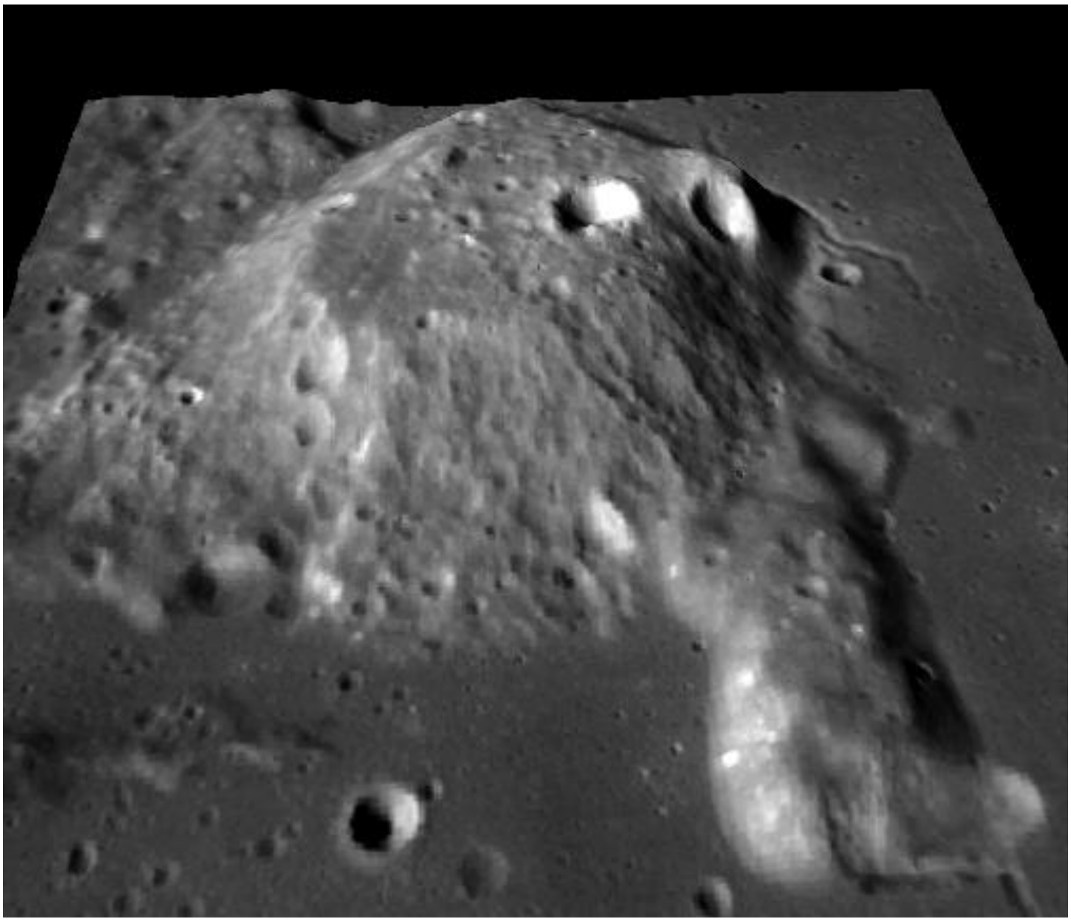

Figure 4: 3D reconstruction obtained with GLD 100 dataset. Highland dome termed G1. Evident complex textures and prominences on the summits.

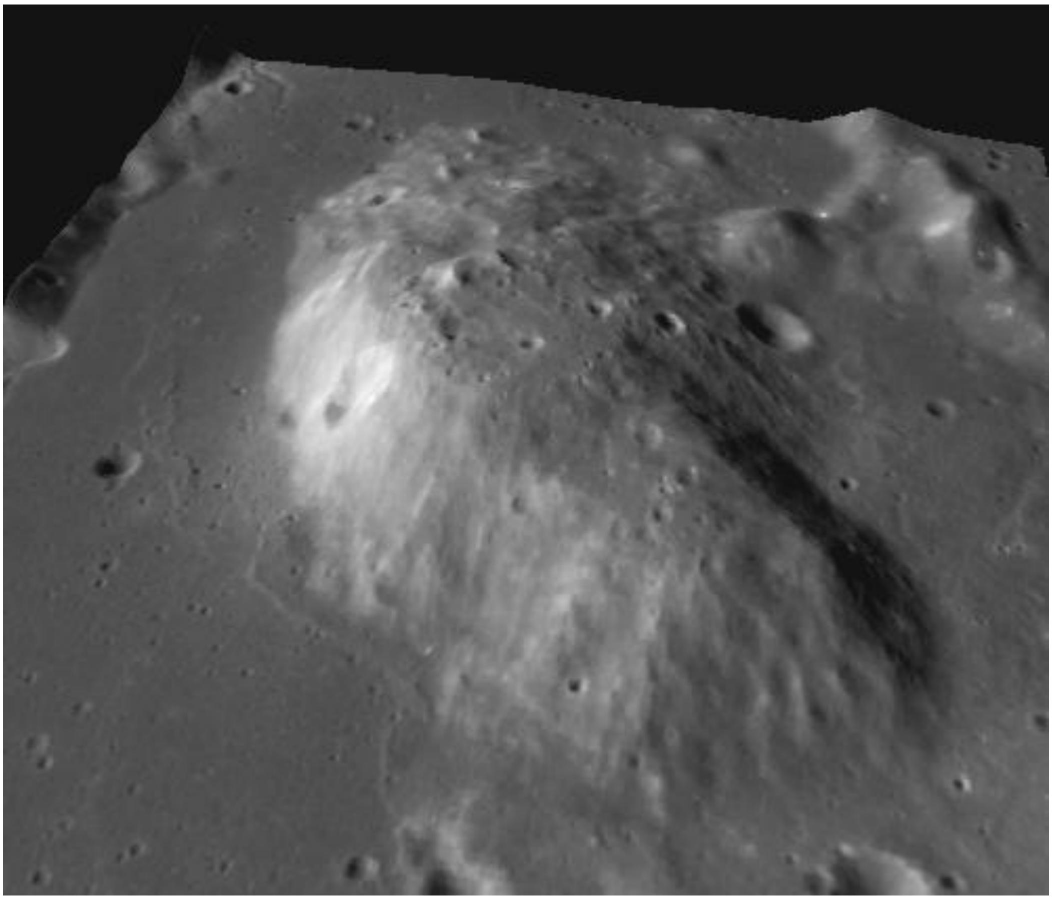

Figure 5: 3D reconstruction obtained with GLD 100 dataset. Highland dome termed G2. Evident complex textures and prominences on the summits.

The Gruithuisen highland domes form a separate spectral and morphometric group (class G) in the lunar domes classification scheme (Lena et al., 2013), due to their steep flank slopes, high volumes, and red spectral signatures, giving rise to the assumption that they have been formed by lava of significantly different composition than basaltic domes and erupted over a long period of time (Lena et al., 2013).

Overview of Mount Amiata

Mount Amiata (with a summit elevation of 1738 m) lies in the southernmost part of Tuscany region in Italy and the surrounding landscape is densely forested and consists of a series of roughly NW-SE trending ridges and valleys. Mount Amiata is a late quaternary complex mainly formed of ignimbrite sheets and trachytic lava domes and flows. It is part of the larger Amiata complex volcano (Fig. 6).

Radiometric dates indicate that the Amiata complex had a major eruptive episode about 300,000 years ago. No eruptive activity has occurred at Amiata during the Holocene, but thermal activity, including cinnabar mineralization, continues at a geothermal field near the town of Bagnore, at the SW end of the dome complex.

Figure 6: Mount Amiata, a panoramic view (photo of Lena).

The activity of Mount Amiata during its main stage consisted of voluminous eruptions of rhyodacitic ignimbrites. This activity was accompanied or followed by the formation of at least seven major lava domes (Fulignati et al., 2014). The latest significant rhyolitic activity in the Mount Amiata area was the emplacement of one large and two smaller flows, the larger one (south of the summit) reaching a length of 5 km while being up to 4 km wide. Smaller flows of more mafic (trachytic) lava were erupted during the last activity, mainly on the eastern flank of the summit lava dome (Figs. 7-8).

Figure 7: Amiata trachytic lava (photo of Lena).

Figure 8: Amiata trachydacitic lava (photo of Lena).

A summary geologic map of the volcanic complex is reported here:
https://www.mdpi.com/energies/energies-07-07434/article_deploy/html/images/energies-07-07434-g001-1024.png

Fulignati et al. (2014) describe a modeling in 3D of Amiata which provides the possibility to interpolate the geometry of structures and the geological features (compare the 3D model with the 3D reconstruction of the highland domes reported above):
https://www.mdpi.com/energies/energies-07-07434/article_deploy/html/images/energies-07-07434-g006-1024.png

The thermal activity with hot springs, and particular concretions of calcium carbonate, is present at Bagni San Filippo (Figs. 9-10).

Figure 9: Bagni San Filippo with thermal activity and hot springs (photo of Lena).

Figure 10: Bagni San Filippo concretions of calcium carbonate (photo of Lena).

Mount Amiata is a relief of a volcanic nature, in which lava activity, about 300,000 years ago, superimposed eruptive rocks and magma flows on a clayey base linked to the evolution of the corrugation of the Apennine chain dating back to the Paleozoic era. To volcanism secondary of Mount Amiata is also the presence of sources of high thermal mineral waters temperature where warm waters over-saturated in calcium bicarbonate rise to the surface. At this neo-tectonic activity could be associated the numerous earthquakes of low magnitude located in the area of Mount Amiata.
Cinnabar is also a mineral of hydrothermal formation (Figs. 11-13), from which mercury is obtained through heating and condensation processes. The common characters in the various fields are the low presence of mercury native, the predominance of cinnabar as the main mineral and the rare association with sulphides.

For about a century (1870-1970) there was an intense industrial extraction of cinnabar, the sulphide from which mercury was obtained, in the Amiata area. For about forty years the mining of cinnabar has been completely abandoned. To remember those events, which were productive, economic and social at the same time, there are now two evocative museums, located one in Abbadia San Salvatore and the other in Santa Fiora.

Figure 11: Cinnabar, Mercury sulfide HgS, in Calcite (private collection of Lena). Cinnabar is generally found in a massive, granular or earthy form and is bright scarlet to brick-red in color.

Figure 12: Cinnabar, Mercury sulfide HgS, in Calcite (private collection of Lena).

Figure 13: Cinnabar (private collection of Lena).

It is also possible to relate to the same genetic process the presence of local antimoniferous mineralization (stibnite), Sb_2S_3 (Fig. 14).

Figure 14: Stibnite, Sb_2S_3, (private collection of Lena).

Mineral microscopy

In the following Figures (Figs. 15-17) are shown some images taken by Heinen using the mineral microscopy (his private collection). A 9Si Leica microscope was used. It has a built-in camera of 10 Mpix. Magnification is from 6.3 to 55X, but can be extended to 110X. Heinen stacks 10 to 40 images using the software HeliconFocus. Images are treated with Lightroom, Sharpen projects pro and Photoshop Elements.

The samples shown in Figs. 15-17 are from Moschellandsberg in Rhenanie-Palatinat, a cryptodome with a lot of different Hg-minerals other than Cinnabar. Moschellandsberg is a rhyolithic laccolith that intruded the surrounding strata during Permian. A rare sulphide mineral containing Copper and Mercury in needle-like is the Gortdrumite $(Cu, Fe)_6 Hg_2S_5$.

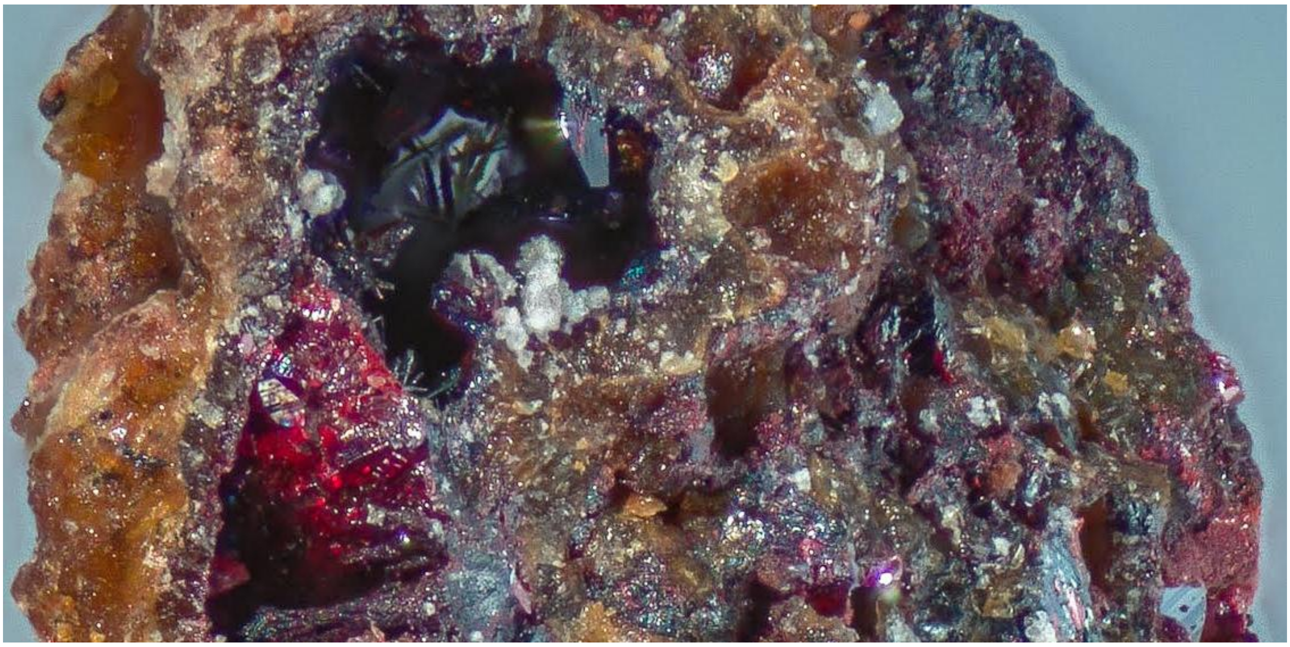

Figure 15: Gortdrumite and Cinnabar 35X, image taken by Heinen from his private collection.

Figure 16: Gortdrumite and Cinnabar (red) 35X, image taken by Heinen from his private collection.

Figure 17: Gortdrumite 50X, a rare sulphide mineral, image taken by Heinen from his private collection.

Domes of trachydacitic and rhyolitic composition

Amiata is a very ancient volcano and site of actual geothermal activity. There are lava domes originating from more viscous lava of a trachytic dacitic composition and with a higher content of silica than the basaltic lavas. There are more than seven of these domes in the Amiata volcanic complex and thus resembling to Gruithuisen highland domes.

Highland lunar domes spectral data

The rheologic modeling analysis by Wilson & Head (2003) yields high viscosities of the lava that formed the lunar highland domes. Diviner dataset produces thermal emissivity data, and can provide compositional information from three wavelengths centered around 8 µm which can be used to characterize the Christiansen Feature (CF), which is directly sensitive to silicate mineralogy and the bulk SiO_2 content. CF value indicates a high Si content of the material that makes up the highland domes Gruithuisen G1-G3, thus supporting their formation by highly viscous lavas. The average calculated CF position for these highland domes is 7.87 µm indicating high plagioclase feldspar composition (Fig. 18).

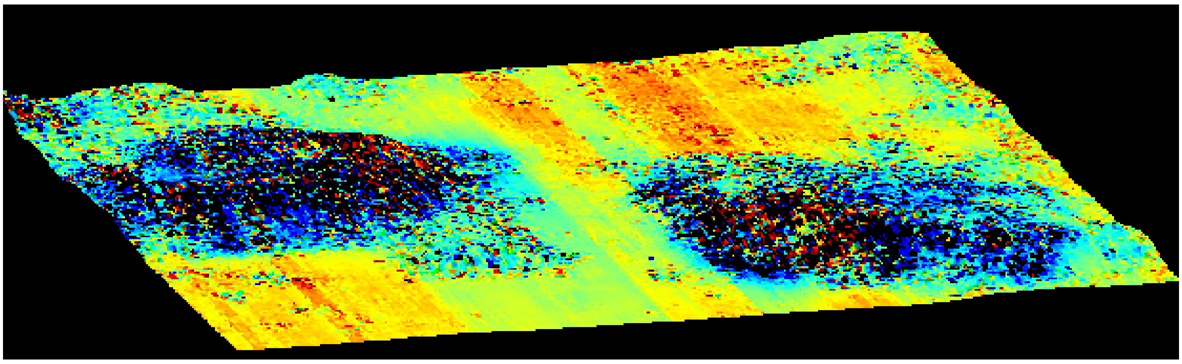

Figure 18: 3D reconstruction of G1 and G2 obtained with GLD 100 dataset overlaid with CF values. Blue color indicates high feldspar composition. The average calculated CF position for these highland domes is 7.87µm.

Recently abundance maps in wt% of Plagioclase, Olivine, Clinopyroxene and Orthopyroxene created from topographically-corrected Mineral Mapper reflectance data acquired by the JAXA SELENE/Kaguya have been released (Fig. 19).

The plagioclase feldspars form a solid solution series between the end members of pure Albite ($NaAlSi_3O_8$) and pure Anorthite ($CaAl_2Si_2O_8$). The alkali feldspars form a solid solution series between pure Albite and Potassium Sanidine ($KAlSi_3O_8$). Astronauts visiting the Moon during the Apollo missions brought back many samples of rock that were rich in feldspar.

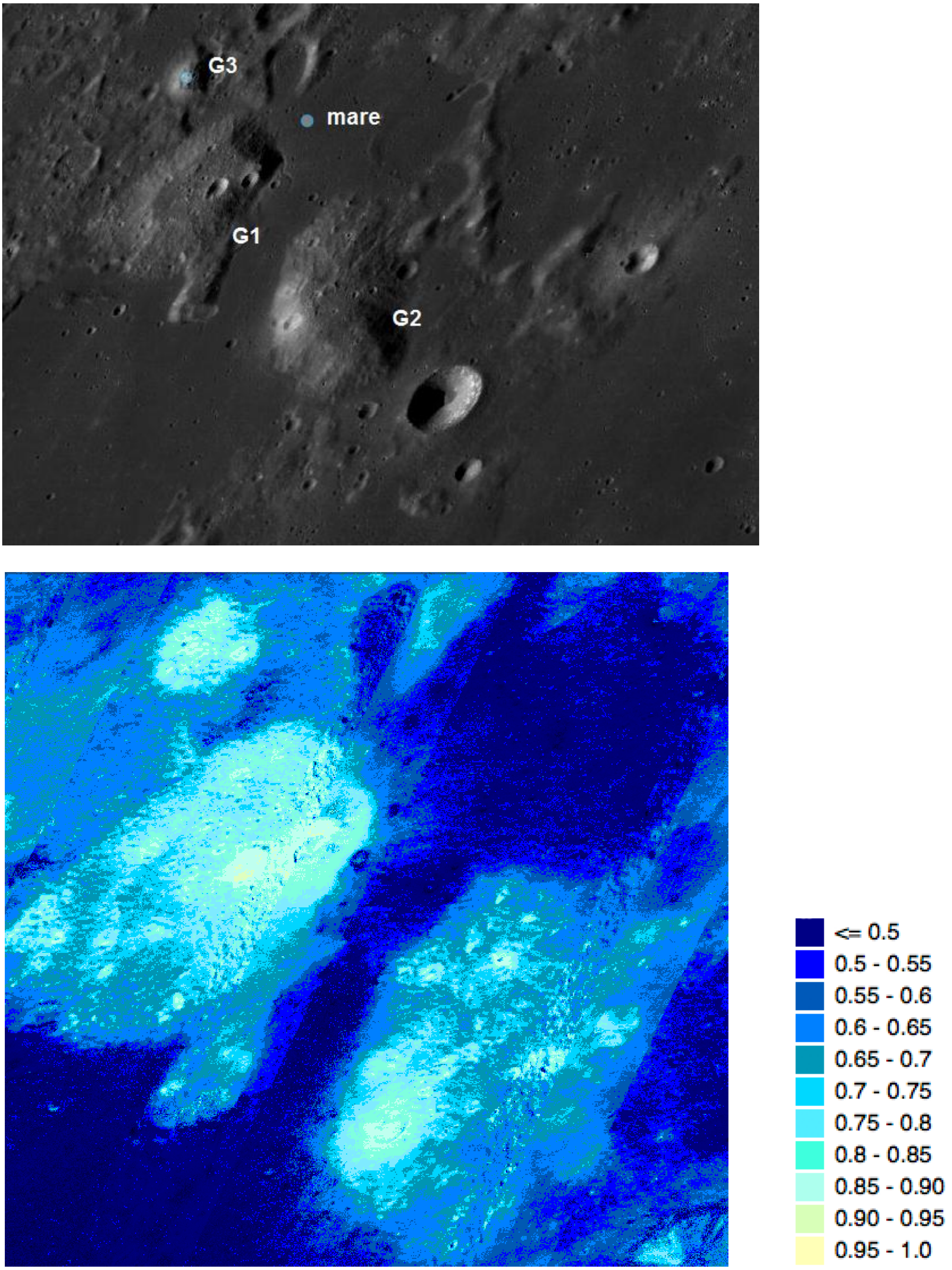

Figure 19: Abundance map in wt% of Plagioclase from Mineral Mapper reflectance data. Note the absence of the plagioclase in the mare and high abundance in the Gruithuisen domes.

Accordingly, the spectral data using Chandrayaan-1 Moon Mineralogy Mapper (M^3) displays a spectrum of the plagioclase which lack any observable mafic absorption feature (Fig. 20) in the range between 1,000 and 2,300 nm. Fig. 20 shows the spectrum of G3 Northwest Dome.
The spectral properties of major lunar minerals exhibit absorption bands that differ by their shape and position along the spectral domain. Pyroxenes (orthopyroxenes and clinopyroxenes) have two absorption bands, one centered near 1,000 nm and another near 2,000 nm. Olivine has a complex absorption centered over 1,000 nm, with no absorption at 2,000 nm. Therefore, olivine-rich lunar deposits are characterized by a broad 1,000 nm absorption band which is enhanced relative to the weak or absent 2,000 nm band.

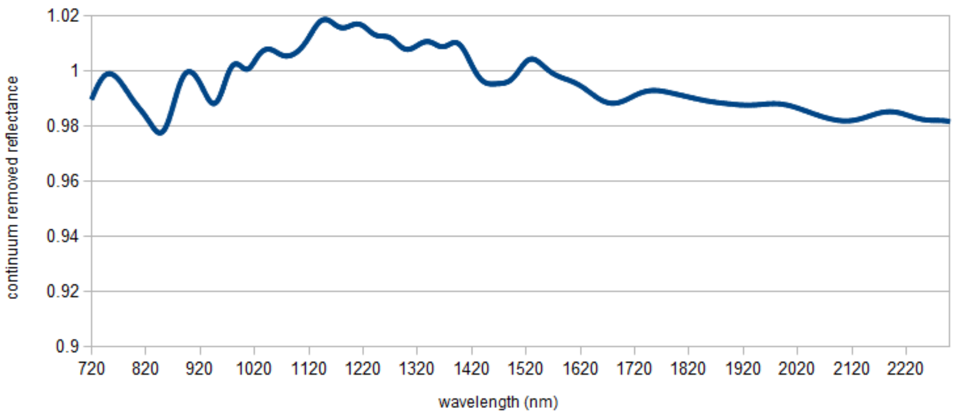

Figure 20: Moon Mineralogy Mapper (M^3) spectrum of G3 Northwest Dome.

Figure 21 displays an olivine component in the mare location marked with a circle in the WAC image of Fig. 19.

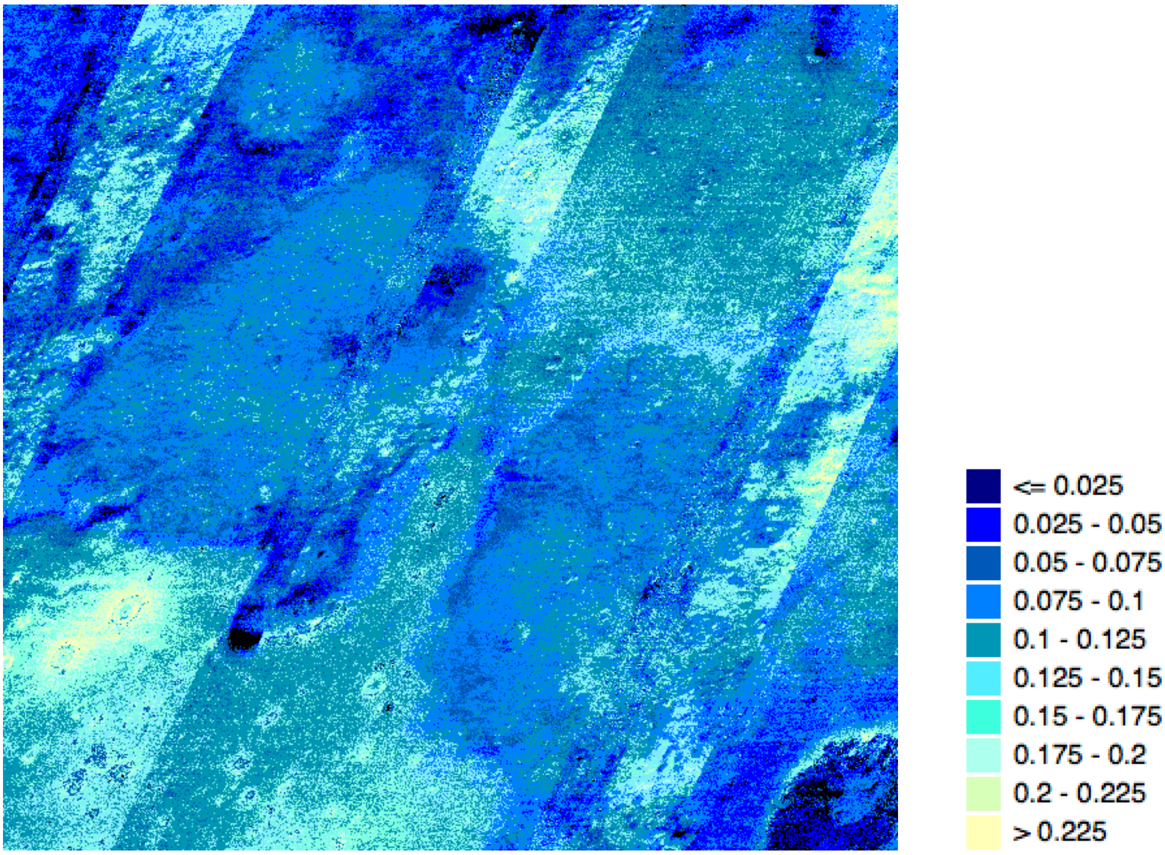

Figure 21: Abundance map in wt% of Olivine from Mineral Mapper reflectance data.

Accordingly, the spectral data using Chandrayaan-1 Moon Mineralogy Mapper (M^3) displays a spectral signature of the olivine (Fig. 22).

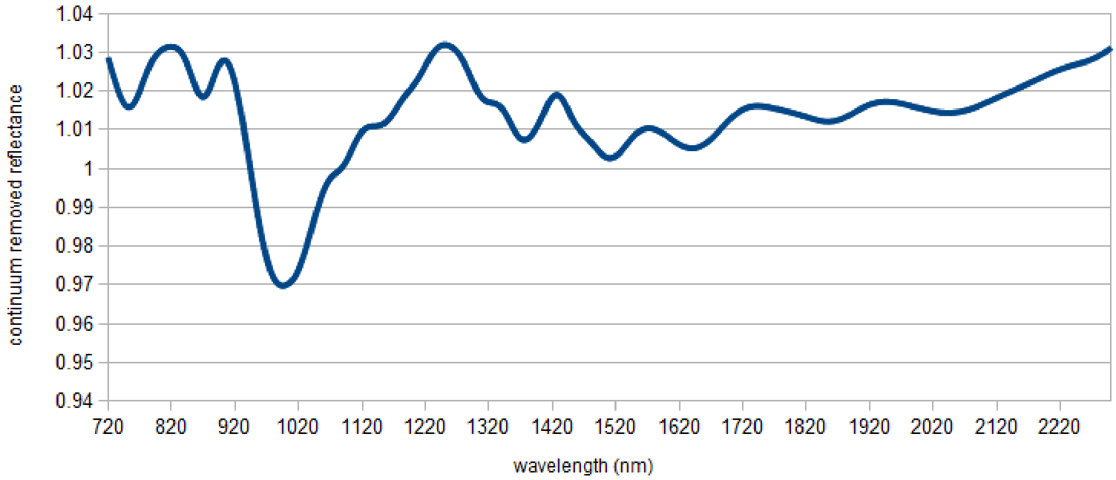

Figure 22: Moon Mineralogy Mapper (M^3) spectrum of the mare near the Gruithuisen highland domes.

As a note of interest, recent detection of water and/or hydroxyl anomaly (OH/H_2O) of endogenic magmatic origin is reported at some highland domes: prominent hydration features have been observed in both Hansteen α and Gruithuisen Domes (Pathak et al., 2015). In Gruithuisen domes, the spectra lack any observable mafic absorption feature, except the absorption OH/H_2O feature near 2,800 nm having band strengths varying from ~5-8%. According to Pathak et al. (2015), I have effectively identified the presence of the hydroxyl group in some areas of Gruithuisen δ (G2) as demonstrated by the spectral signature, characterized by the 2,800 nm spectral absorption very diagnostic (Fig. 23).

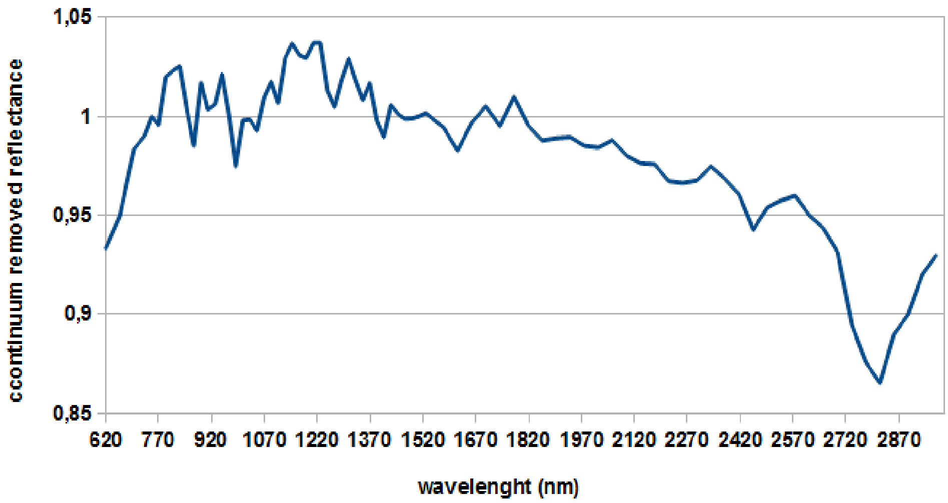

Figure 23: M^3 spectral analysis of the dome Gruithuisen δ (G2).

The observed hydroxyl (OH/H_2O) feature at this non-mare silicic lithology indicates the presence of endogenic magmatic water. The dissolved water in silicates changes their physical and chemical properties as they can alter their structure, and thus plays a crucial role in volcanic eruptions and affects the evolution of magma.

References

Biagioni, C., Musetti, S., Pasero, M. New Data on Metacinnabar from Tuscany (Italy) Atti Soc. Tosc. Sci. Nat., Mem., Serie A, 124 (2017) pagg. 13-18, doi: 10.2424/ASTSN.M.2017.14 https://arpi.unipi.it/retrieve/handle/11568/897286/332502/BIAGIONI_897286.pdf

Chevrel, S.D., Pinet, P.C., Head, J.W., 1999. Gruithuisen domes region: A candidate for an extended nonmare volcanism unit on the Moon. J. Geophys Res. 104 (E7), 16515–16529.

Fulignati P, Marianelli P, Sbrana A, Ciani V. 3D Geothermal Modelling of the Mount Amiata Hydrothermal System in Italy. *Energies*. 2014; 7(11):7434-7453.

Greenhagen, B.T., Lucey, P. G., Wyatt, M.B., Glotch, T. D., Allen,C.C., Arnold, J. A., Bandfield, J. L., Bowles, N. E., Donaldson Hanna, K. L., Hayne, P. O., Song, E., Thomas, I. R., Paige, D. A., 2010. Global Silicate Mineralogy of the Moon from the Diviner Lunar Radiometer. Science, 329, 1507-1509. Doi: 10.1126/science.1192196

Lena, R., Wöhler, C., Phillips, J., Chiocchetta, M.T., 2013. Lunar domes: Properties and Formation Processes, Springer Praxis Books.

Pathak, S., Basantaray, A.K., Chauhan, M., Bhattacharya, S. and Chauhan, P., Endogenic Water/Hydroxyl Anomaly Associate With Lunar Silicic Domes Detected by Chandrayaan-1 Moon Mineralogy Mapper (M^3) Instrument and its Implications. 46th Lunar and Planetary Science Conference (2015). Abstract# 1400.

Wilson, L., Head, J.W., 2003. Lunar Gruithuisen and Mairan domes: rheology and mode of emplacement. J. Geophys. Res. 108 (E2), 5012–5018.

Wohletz, Kenneth, and Grant Heiken. Volcanology and Geothermal Energy. Berkeley: University of California Press, 1992. http://ark.cdlib.org/ark:/13030/ft6v19p151/